2016

Intra-Storm Temporal Patterns of Rainfall in China Using Huff Curves

Shui-qing Yin
Beijing Normal University

Yun Xie
Beijing Normal University

Mark A. Nearing
United States Department of Agriculture

Wen-li Guo
Beijing Meteorology Bureau

Zhengyuan Zhu
Iowa State University, zhuz@iastate.edu

Intra-Storm Temporal Patterns of Rainfall in China Using Huff Curves

Abstract
Intra-storm temporal distributions of precipitation are important for infiltration, runoff, and erosion process understanding and models. A convenient and established method for characterizing precipitation hyetographs is the use of non-dimensional Huff curves. In this study, 11,801 erosive rainfall events with 1 min resolution data collected over 30 to 40 years from 18 weather stations located across the central and eastern parts of China were analyzed to produce Huff curves. Each event was classified according to the quartile period within the event that contained the greatest fraction of rainfall. The results showed that 38.3% of events had the maximum rainfall amounts in the first quartile, followed by the second (26.8%), third (22.4%), and fourth (12.5%) quartiles. Quartile I and II events were generally characteristic of shorter duration and heavier intensity events. Quartile I events averaged 23% shorter durations than quartile IV events, whereas the mean intensity (Iavg), mean maximum 30 min intensity (I30), and mean rainfall erosivity index (EI30) were 1.71, 1.22, and 1.23 times greater, respectively, than those for quartile IV and were significant at a 5% level based on two-sample t-tests. The proportion of quartile I events was less for events of longer duration, whereas the proportions of quartile III and IV events were greater. Two-sample Kolmogorov-Smirnov tests suggested that regional Huff curves can be derived for the central and eastern parts of China. Regional Huff curves developed in this study exhibited dissimilarities in terms of the percentages of storms for different quartiles and the shapes of the curves compared to those reported for Illinois, peninsular Malaysia, and Santa Catarina in Brazil.

Keywords
Duration, Erosive, Hyetograph, Intensity, Precipitation, Rainfall, Storm

Disciplines
Atmospheric Sciences | Earth Sciences | Environmental Monitoring | Longitudinal Data Analysis and Time Series | Statistics and Probability

Comments
This article is published as Yin, Shui-qing, Yun Xie, Mark A. Nearing, Wen-li Guo, and Zheng-yuan Zhu. "Intra-Storm Temporal Patterns of Rainfall in China Using Huff Curves." *Transactions of the ASABE* 59, no. 6 (2016): 1619-1632. DOI: 10.13031/trans.59.11010. Posted with permission.

INTRA-STORM TEMPORAL PATTERNS OF RAINFALL IN CHINA USING HUFF CURVES

S.-q. Yin, Y. Xie, M. A. Nearing, W.-l. Guo, Z.-y. Zhu

ABSTRACT. *Intra-storm temporal distributions of precipitation are important for infiltration, runoff, and erosion process understanding and models. A convenient and established method for characterizing precipitation hyetographs is the use of non-dimensional Huff curves. In this study, 11,801 erosive rainfall events with 1 min resolution data collected over 30 to 40 years from 18 weather stations located across the central and eastern parts of China were analyzed to produce Huff curves. Each event was classified according to the quartile period within the event that contained the greatest fraction of rainfall. The results showed that 38.3% of events had the maximum rainfall amounts in the first quartile, followed by the second (26.8%), third (22.4%), and fourth (12.5%) quartiles. Quartile I and II events were generally characteristic of shorter duration and heavier intensity events. Quartile I events averaged 23% shorter durations than quartile IV events, whereas the mean intensity (I_{avg}), mean maximum 30 min intensity (I_{30}), and mean rainfall erosivity index (EI_{30}) were 1.71, 1.22, and 1.23 times greater, respectively, than those for quartile IV and were significant at a 5% level based on two-sample t-tests. The proportion of quartile I events was less for events of longer duration, whereas the proportions of quartile III and IV events were greater. Two-sample Kolmogorov-Smirnov tests suggested that regional Huff curves can be derived for the central and eastern parts of China. Regional Huff curves developed in this study exhibited dissimilarities in terms of the percentages of storms for different quartiles and the shapes of the curves compared to those reported for Illinois, peninsular Malaysia, and Santa Catarina in Brazil.*

Keywords. *Duration, Erosive, Hyetograph, Intensity, Precipitation, Rainfall, Storm.*

Temporal scales relevant to many earth surface processes, such as infiltration, runoff, and erosion, are short, with intra-storm rainfall intensity variations being important. Therefore, process-based hydrological and erosion models often require high temporal resolution precipitation data. Coarser data, such as daily or even monthly time scales, often lead to poor model performance (Yu et al., 1997; Kandel et al., 2004). However, fine-scale hydrometeorological data are not widely and readily available. As a result, statistically representative, synthetic storms are often used. The SWIM (Soil Water Infiltration and Movement; Ross, 1990) and WEPP (Water Erosion Prediction Project; Lane and Nearing, 1989) models have the capability to use a weather generator, which can be used to simulate within-storm characteristics stochastically based on the statistics of historical weather sequences or other information (e.g., temporally downscaled projected climate regimes).

Artificial storms generated by a rainfall simulator in field experiments have shown that the patterns of rainfall intensity within the event lead to different results for runoff and erosion. Flanagan et al. (1988) used a rainfall simulator to study storm pattern effects on a silt loam, cropland soil in Indiana. They demonstrated that when artificial storms were applied to the dry soil, peak runoff rates were 4 to 20 times greater, and soil loss was 2 to 8 times greater, for the events having maximum intensities in the last quartile of the event compared to those peaking in the early stages. Durkerley (2012) applied a series of events on bare, crusted dryland soils. Each event had a duration of 90 min, mean intensity of approximately 10 mm h^{-1}, and total rainfall depth of 15 mm. Four different event profiles, including uniform, early peak, late peak, and early peak-gap, were classified. The event profiles had a principal intensity peak of 30 mm h^{-1} and a secondary intensity peak of 15 mm h^{-1}. The results showed that runoff ratios and peak runoff rates were 85% to 570% greater than measured values for the experiments with varying intensity compared to those with uniform intensity. For these reasons, the intra-storm temporal characteristics of rainfall are needed and are important for driving process-based hydrologic and erosion models in order to represent natural rainfall processes.

Considerable research has been conducted on the time distributions of storms (Keifer and Chu, 1957; Hershfield, 1962; Huff, 1967; Pilgrim and Cordery, 1975; Yen and

Submitted for review in October 2014 as manuscript number NRES 11010; approved for publication by the Natural Resources & Environmental Systems Community of ASABE in October 2016.

Mention of company or trade names is for description only and does not imply endorsement by the USDA. The USDA is an equal opportunity provider and employer.

The authors are **Shui-qing Yin,** Associate Professor, and **Yun Xie,** Professor, State Key Laboratory of Earth Surface Processes and Resource Ecology and School of Geography, Beijing Normal University, Beijing, China; **Mark A. Nearing,** Research Agricultural Engineer, USDA-ARS Southwest Watershed Research Center, Tucson, Arizona; **Wen-li Guo,** Professor, Beijing Climate Center, Beijing Meteorology Bureau, Beijing, China; **Zheng-yuan Zhu,** Associate Professor, Department of Statistics, Iowa State University, Ames, Iowa. **Corresponding author:** Shui-qing Yin, Xin-Jie-Kou-Wai Street, Haidian district, Beijing, 100875 China; phone: 0086-10-58807455-1687; e-mail: yinshuiqing@bnu.edu.cn.

Chow, 1980; Terranova and Iaquinta, 2011). Four types of dimensionless hyetograph curves (types I, IA, II, and III) were developed by the USDA Soil Conservation Service (now the Natural Resources Conservation Service) (USDA, 1986). Huff (1967) proposed the concept of a dimensionless cumulative distribution curve of normalized accumulated rainfall as a function of normalized rainfall duration. Using this concept, he classified storms as first, second, third, or fourth quartile (quartiles I, II, III, and IV) according to the quartile of the storm duration where the greatest percentage of cumulative rainfall, and hence average rainfall intensity, occurred.

Design storms developed using the Huff curve method differ from those developed by other procedures. Bonta (2004a) showed that the Huff curves did not correspond to the NRCS design storm curves. Azli and Rao (2010) demonstrated significant differences between the Huff curves and the design storm developed for peninsular Malaysia as reported in the Urban Stormwater Management Manual for Malaysia. Bonta and Rao (1988a) compared four different procedures for defining a design storm and concluded that the procedure of Huff (1967) was the most flexible. Huff (1990) reported that quartile I events often had durations of 6 h or less and quartile II events had durations of 6 to 12 h. Based on this, it was suggested that for hydraulic design applications, hyetographs for quartile I should be used for time scales of no more than 6 h and quartile II for 6 to 12 h. Hjelmfelt (1980) introduced Huff curves into a field-scale model for CREAMS (Chemicals, Runoff, and Erosion from Agriculture Management Systems) and recommended that the 50% probability curve be used.

Huff curves are not only useful for determining design storms but also for stochastic intra-storm simulation. Bonta (2004a) concluded that Huff's method has the following advantages as a procedure for rainfall storm generation: (1) hourly precipitation data gave nearly identical Huff curves as 3 min data, which suggested that the more widely available hourly data can be used to obtain Huff curves and generate intra-storm patterns to drive hydrologic and erosion models, such as SWIM (Ross, 1990) and WEPP (Lane and Nearing, 1989); (2) Huff curves appear relatively insensitive to the minimum dry period duration (MDPD) used to delineate individual storms; (3) there was relatively good stability with change of storm sample size; and (4) there was similarity between Huff curves developed over relatively long distances, which suggests potential for regionalization according to broad climatic regimes. Bonta (2004b) proposed a stochastic simulation method for within-storm intensities that used the probabilistic information contained in Huff curves.

Huff curves have been developed by scientists from other areas in the world, such as the U.K. (NERC, 1975), southwestern British Columbia in Canada (Loukas and Quick, 1996), Oman (Al-Rawas and Valeo, 2009), Malaysia (Azli and Rao, 2010), and Santa Catarina State in Brazil (Back, 2011). As recognition of the utility of Huff curves, the National Oceanic and Atmospheric Administration (NOAA) released Huff curves for different areas of the U.S. (Bonnin et al., 2006, 2011; Perica et al., 2013a, 2013b, 2014). Many studies have confirmed that the differences among Huff curves over long distances in the same climatic region are often minor. Loukas and Quick (1996) compared Huff curves within the same climatic region in coastal British Columbia, Canada, and reported that the time distribution of the storms was similar regardless of the elevation, type of storm, storm duration, or storm precipitation depth. Al-Rawas and Valeo (2009) found that the differences between the mountainous and coastal regions were minor within arid Oman, where the annual rainfall ranged from 100 to 350 mm. The differences between Huff curves for Oman and Calgary (in Alberta, Canada) were also small. It was demonstrated that Huff curves from 13 stations in peninsular Malaysia were similar (Azli and Rao, 2010). Averaged Huff curve sets in peninsular Malaysia were also compared to those derived from 6 h storms in the Midwestern U.S. (Bonnin et al., 2006), and it was indicated that Huff curves for the third and fourth quartiles were similar, whereas those for the first and second quartiles were not.

In China, the design storm hyetograph pattern is often characterized using a subjectively selected typical storm from observational data and rescaling according to an intensity-duration-frequency relationship. Two design storm definition methods developed by Wang (2002) appear to be able to reduce the subjectivity by considering a larger storm sample number (Wang, 1994; Wu, 2002). Research on Huff curves has been limited in China. The design rainfall distribution for Tianjin city was developed using Huff's method (Fan, 2011); however, the characteristics of intra-storm variations across China have not been determined.

The hypothesis of the current study is that regionalized patterns of intra-storm rainfall distributions can be found over the central and eastern parts of China. We report here analyses of historic, high temporal resolution rainfall data using the Huff method from 18 stations, synthesize the results, and compare them to published information from other parts of the world. These results have the potential to provide a basis for defining engineering design storms, intra-storm stochastic simulation, and experimental designs for rainfall simulation studies.

DATA AND METHODS

DESCRIPTION OF DATA

One-minute resolution rainfall data were collected from 18 weather stations distributed over the central and eastern parts of China (fig. 1, table 1). The 1 min resolution data were determined by scanning the precipitation pluviograph paper chart from a siphon self-recording rain gauge and converting the precipitation curve to a precipitation amount per minute (Wang et al., 2004). Depth resolution of the data was 0.1 mm. Data were collected from 1961 through 2000 for 16 stations and from 1971 through 2000 for the Wuzhai (53663) and Yangcheng (53975) stations in Shanxi province. The stations covered latitude from 25.0° N to 49.2° N, longitude from 98.5° E to 128.7° E, and elevation from 20.6 to 1896.8 m. The distance between station pairs ranged from 70.9 to 3559.8 km with a mean of 626.2 km. For the northern stations, the total rainfall during May through September (thus excluding snow events) ranged from 353.8 to 551.3 mm. For the ten stations in the southern snowless ar-

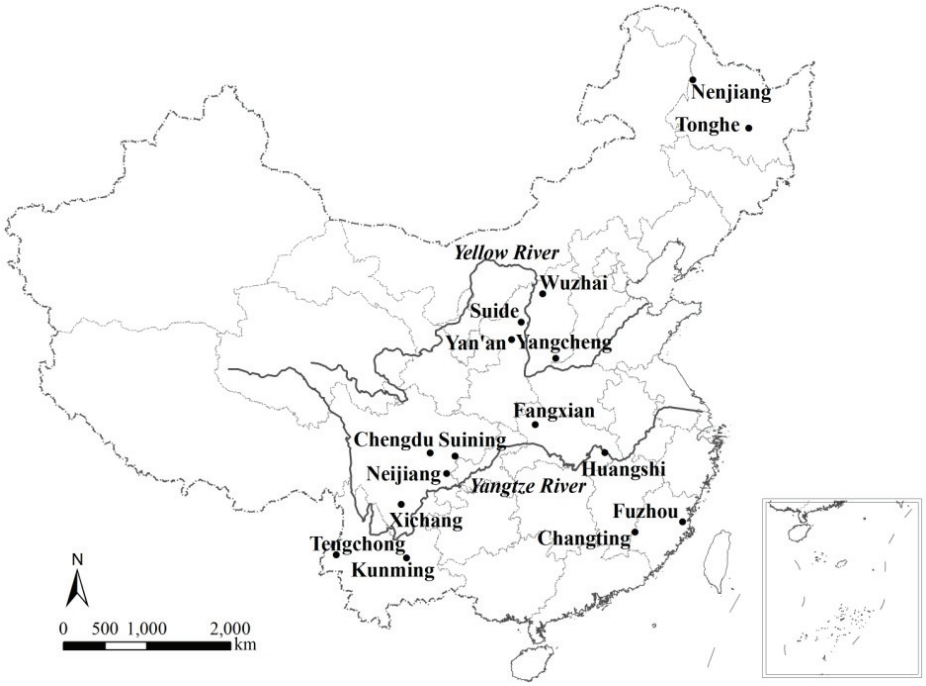

Figure 1. Distribution of the 18 meteorological stations with 1 min temporal resolution rainfall data used in this study.

Table 1. Meteorological stations used.

Province	Station No.	Station Name	Latitude (°N)	Longitude (°E)	Altitude (m)	Annual Rainfall[a] (mm)	No. of Events
Heilongjiang	50557	Nenjiang	49.17	125.23	243	419.3	343
	50963	Tonghe	45.97	128.73	110	479.9	471
Shanxi	53663	Wuzhai	38.92	111.82	1402	360.4	289
	53975	Yangcheng	35.48	112.4	658.8	435.8	340
Shaanxi	53754	Suide	37.5	110.22	928.5	353.8	256
	53845	Yan'an	36.6	109.5	958.8	409.2	411
Beijing	54416	Miyun	40.38	116.87	73.1	551.3	476
	54511	Guanxiangtai	39.93	116.28	54.7	494.4	434
Sichuan	56294	Chengdu	30.67	104.02	506.1	853.4	717
	56571	Xichang	27.9	102.27	1590.9	975.7	998
	57405	Suining	30.5	105.58	279.5	902.1	654
	57504	Neijiang	29.58	105.05	352.4	988.2	826
Hubei	57259	Fangxian	32.03	110.77	427.1	712.3	563
	58407	Huangshi	30.25	115.05	20.6	1248.6	898
Yunnan	56739	Tengchong	25.02	98.5	1648.7	1393.6	1205
	56778	Kunming	25.02	102.68	1896.8	905.5	747
Fujian	58847	Fuzhou	26.08	119.28	84	1338.2	1136
	58911	Changting	25.85	116.37	311.2	1590.7	1037

[a] For the eight stations located in the northern part of the study area, including Nenjiang, Tonghe, Wuzhai, Yangcheng, Suide, Yan'an, Miyun and Guanxiangtai, annual rain refers to the sum of rainfall during May through September.

eas, the mean annual rainfall varied from 712.3 to 1590.7 mm.

Huff curves appear relatively insensitive to changes in MDPD (Bonta and Rao, 1987). An individual rainfall event was defined as a period of rainfall with at least six preceding and six succeeding non-precipitation hours, following Huff (1967), in order to facilitate comparison of Huff curves for different areas of the world. Only erosive events with rainfall amounts equal to or greater than 12 mm were analyzed in this study (Xie et al., 2002). The number of events ranged from 256 to 1205 among the 18 stations, with a total of 11,801 events (table 1). The minimum number of within-storm data points for each storm used was 20 records.

For the eight stations in the northern part of the study area, only the period from May through September was used because the rain gauges were out of service to avoid freeze damage in winter. However, based on daily data from simpler rain gauge types with year-round observations, rainfall during May through September for these eight northern stations represented 76% to 87% of total annual precipitation, including 84% to 95% of the total erosive rainfall (summation of daily rainfall equal to or greater than 12 mm).

Determination of Huff Curves for Point Rainfall

The procedures for defining rainfall types and drawing Huff curves were identical to those used by Huff (1967) and were described in detail by Bonta (2004a):

1. Obtain total rainfall depth (A, mm), total duration (D, min), cumulative rainfall depth for the rth minute (A_r, mm), and cumulative duration for the rth minute

(D_r, min). When $D_r = 0$, then $A_r = 0$, and when $D_r = D$, then A_r = A. Each event is non-dimensionalized by dividing cumulative rainfall depth by the total depth and dividing cumulative duration by the total duration:

$$p_r = \frac{A_r}{A} \tag{1}$$

$$t_r = \frac{D_r}{D} \tag{2}$$

2. For each event, values of $t_r = j$ (j = 0, 0.1, 0.2, …, 0.8, 0.9, 1) are identified or interpolated from the data with corresponding values of $p_j = p_r$. The value of p_j represents the non-dimensional cumulative rainfall depth at non-dimensional time j in the event.

3. For a location with a total of n events (for example, n = 343 for Nenjiang station in Heilongjiang province), there are n sample points for each non-dimensional data pair (j, p_j). For each value of j (j = 0.1, 0.2,…, 0.8, 0.9), the n number of p_j values are sorted in descending order to obtain a series $(p_j)_i$ (i = 1, 2, …, n). From this series, the empirical probability of exceedance value, f (%), for any value of $(p_j)_i$ is calculated as:

$$f = \frac{100i}{n+1} \tag{3}$$

$$i(f) = \left[\frac{f(n+1)}{100} \right] \tag{4}$$

4. Determine the value of $(p_j)_{i(f)}$ for exceedance probabilities (f = 10, 20, …, 80, 90) using equations 3 and 4. Do this for each of the nine values of j (j = 0.1, 0.2, …, 0.8, 0.9). Note that (x_j, p_j) = (0, 0) for j = 0, and (x_j, p_j) = (1, 1) for j = 1.

5. For each value of f (f = 10, 20, …, 80, 90), draw a curve (isopleth) connecting points j, $(p_j)_{i(f)}$. The nine resulting isopleths are the Huff curves, which are a "probabilistic summary representation of storm mass curves in terms of dimensionless elapsed times into a storm and corresponding dimensionless accumulated depths" (Bonta, 2004a).

The above method was used to generate the nine Huff curves for all storm types at each location, which means the curves developed in this study were "point-developed" Huff curves. For looking at different quartile classifications of peak intensities, each storm was divided into quartiles of equal duration and then classified as quartiles I, II, III, or IV according to the quartile in which the greatest percentage of cumulative rainfall occurred. We then selected all events for each specific quartile and followed the steps above to obtain the nine Huff curves (representing the nine probability levels) for each of the four quartile storm types, thus obtaining 36 Huff curves for each station, i.e., nine for each of the four storm types, as suggested by Huff (1967).

Statistical Tests Used in the Comparison

A two-sample Kolmogorov-Smirnov (KS) test was used to test for statistically significant differences between the Huff curves among the 18 stations (Bonta and Shahalam, 2003). Pairs of stations were compared in each test, and there were 153 pairs of stations in total. For each pair of stations and for each duration value of j (j = 0.1, 0.2,…, 0.8, 0.9), the KS test compared two independent cumulative frequency distributions of p_j. Therefore, there were nine KS tests for each pair of stations and 5508 tests (9 points of dimensionless duration × 153 pairs of stations × 4 storm types) for the four quartile types of Huff curves. Pearson correlation coefficients were calculated to detect correlations between the p-values of KS tests for station pairs and their distances and to detect if stations closer to each other share more similarities (Snedecor and Cochran, 1989).

A method based on a bootstrap scheme was designed to test differences between the Huff curves developed in this study and those reported for Illinois (Huff, 1990), peninsular Malaysia (Azli and Rao, 2010), and Santa Catarina in Brazil (Back, 2011). The climate of north China is categorized as humid continental (Dfa) according to Köppen climate classification with hot, humid summers, whereas south China is humid subtropical (Cfa) with hot, muggy summers and frequent thunderstorms. Similar to north China, Illinois is classified as Dfa, while peninsular Malaysia is tropical rainforest (Af) with evenly distributed, heavy precipitation throughout the year, and Santa Catarina in Brazil is tropical monsoon (Am) with heavy rain in the wet season and strong sun in the dry season. Note that Huff curves have been developed both from point rainfall and over areas (Huff, 1990), and we compared only the point-developed curves. The bootstrap scheme involves random sampling with replacement, which means that some storms may be sampled more than once. The distance between station pairs in this study ranged from 70.9 to 3559.8 km with a mean of 626.2 km. The storm samples from different stations can be assumed to be independent because the stations were so distant from each other. Note that the number of resampled storms is equal to the number of observed storms. Huff curves were determined using the procedure described in the previous section for each bootstrap resample. Taking quartile I and f = 10% as an example, for each value of j (j = 0.1, 0.2, …, 0.8, 0.9), $(p_{j,m,k})_{i(f)}$ represents the $(p_j)_{i(f)}$ value for the mth station and the kth bootstrap resample (we repeated bootstrap resampling 500 times in this study). For simplicity, exceedance probability $i(f)$ is omitted in the following denotations. The mean ($\bar{p}_{j,m}$) and standard error ($s_{j,m}$) for 500 resamplings can be estimated as follows:

$$\bar{p}_{j,m} = \frac{1}{500} \sum_{k=1}^{500} p_{j,m,k} \tag{5}$$

$$s_{j,m} = \sqrt{\frac{1}{500-1} \sum_{k=1}^{500} (p_{j,m,k} - \bar{p}_{j,m})^2} \tag{6}$$

The mean ($\bar{p}_j$) and standard error (s_j) for all 18 stations were calculated using equations 7 and 8. The overall standard deviation (s'_j) included the deviation among the 18 stations (s_j) and the average value of the deviation for each station ($s_{j,m}$), which was estimated using equation 9:

$$\bar{p}_j = \frac{1}{18}\sum_{m=1}^{18} \bar{p}_{j,\,m} \tag{7}$$

$$s_j = \sqrt{\frac{1}{18-1}\sum_{m=1}^{18} (\bar{p}_{j,m} - \bar{p}_j)^2} \tag{8}$$

$$s'_j = s_j + \frac{1}{18}\sum_{m=1}^{18} s_{j,\,m} \tag{9}$$

The confidence interval was calculated as:

$$\left[\bar{p}_j - 1.96\frac{s'_j}{\sqrt{18}}, \bar{p}_j + 1.96\frac{s'_j}{\sqrt{18}}\right] \tag{10}$$

and $u_{j,a}$ is the dimensionless depth at j (j = 0.1, 0.2, …, 0.8, 0.9) for three regions (a = 1, 2, 3). If $u_{j,a}$ is in the confidence interval, there is no statistically significant difference between $\bar{p}_j$ and $u_{j,a}$ at a significance level of $\alpha = 0.05$. Otherwise, there is significant difference between them. There were nine tests for each pair of curves. In total, there were 324 tests (9 points of dimensionless duration × 3 probabilities × 4 storm types × 3 regions) for three probabilities (10%, 50%, and 90%) and four quartile types.

The reason for using the KS test and bootstrap-based test is that they are more general and require less restrictive assumptions. Conventional variance testing is based on large sample theory and asymptotic approximation and works well for comparing means of distributions when the sample size is reasonably large and the distribution is normal. However, it does not work well when we are comparing more extreme quantiles and when the assumptions on sample size and distribution do not hold. The KS test is distribution-free and compares the cumulative distribution of two datasets but is not limited to comparison of the means. Bootstrap-based test results are similar to conventional test results when those assumptions hold and perform better than conventional tests when the sample distribution deviates from the normal distribution.

Effect of Duration and Season on Huff Curves

In addition to developing Huff curves based on all storms for each station, Huff curves were also developed for different duration groups and different seasons. For duration groups, the events across all seasons (through the entire year) were divided into six groups according to their duration: up to 6 h, 6 to 12 h, 12 to 18 h, 18 to 24 h, 24 to 48 h, and more than 48 h. Huff curves were developed for each group of data and peak intensity quartile. Next, the events in summer only (June through August) were similarly divided into the same six groups because most rainfall occurred in summer and storm sample numbers were sufficient for each group for the summer season. That was not true for the other three seasons. Thus, for seasonal analysis, all the events (across all durations) were divided by season, including spring, summer, autumn, and winter, which included March through May, June through August, September through November, and December through February, respectively. For assessing the seasonal trends, all the stations were combined by season. The effects of duration and season on Huff curves pattern were determined by the KS test described in the previous section.

Five indices were investigated to characterize each quartile classification of rain, including storm amount, duration, average intensity (I_{avg}), maximum 30 min intensity (I_{30}), and rainfall erosivity index (EI_{30}), which is the multiplication of rainfall energy and maximum 30 min intensity. EI_{30} is an important index in the empirical soil loss prediction model, the Universal Soil Loss Equation (USLE), and its successors (RUSLE, RULSE2) (Wischmeier and Smith, 1978; Renard et al., 1997; Foster, 2004). Two-sample t-tests were used to test the differences in averaged indices from different quartiles (Snedecor and Cochran, 1989).

Results

Development of Regional Huff Curves for the Four Storm Quartile Types

Quartile I, with 4516 out of 11801 events (38.3%), was the most frequent storm type found at all stations, followed by quartiles II (3167 events, 26.8%), III (2646 events, 22.4%), and IV (1472 events, 12.5%) in descending order (table 2). Most of the events belonged to quartiles I and II, which together represented 65.1% of total erosive events.

Figure 2 shows all the curves of the 10%, 50%, and 90% isopleths for each storm quartile type. Curves for quartile IV visibly showed more variation between stations than the curves for the other quartiles, probably due to its smaller sample sizes. The 10% exceedance curve for quartile IV for Wuzhai station (shown with circles in fig. 2d) visually appeared to be quite different from those for the other stations. There were only 35 erosive events belonging to quartile IV for the Wuzhai station, which may have led to a poor definition of that curve.

KS tests that compared all possible pairings of the stations showed that 61.0%, 60.5%, 69.9%, and 69.9% of the station pairs were from the same distribution (fig. 3) for quartiles I, II, III, and IV, respectively. The percentage of station pairs

Table 2. Percentage of each storm peak quartile type for the 18 stations. Events were classified into four types by the storm duration quartile of maximum rainfall.

	Quartile				
Station	I	II	III	IV	I + II
Nenjiang	37.9	21.3	26.2	14.6	59.2
Tonghe	41.2	23.8	20.4	14.6	65.0
Wuzhai	34.6	30.4	22.8	12.1	65.1
Yangcheng	40.6	25.0	23.8	10.6	65.6
Suide	30.9	32.4	24.2	12.5	63.3
Yan'an	41.4	24.1	23.4	11.2	65.5
Miyun	38.4	28.8	19.5	13.2	67.2
Guanxiangtai	36.6	24.9	24.9	13.6	61.5
Chengdu	43.1	26.6	19.8	10.5	69.7
Xichang	47.2	27.9	16.9	8.0	75.1
Suining	41.4	26.5	21.6	10.6	67.9
Neijiang	44.9	28.1	18.8	8.2	73.0
Fangxian	42.5	25.0	20.8	11.7	67.5
Huangshi	31.3	29.4	26.5	12.8	60.7
Tengchong	35.2	26.0	22.7	16.2	61.2
Kunming	41.8	24.9	18.7	14.6	66.7
Fuzhou	31.9	27.7	27.2	13.2	59.6
Changting	31.1	27.9	26.0	14.9	59.0
Average	38.3	26.8	22.4	12.5	65.1

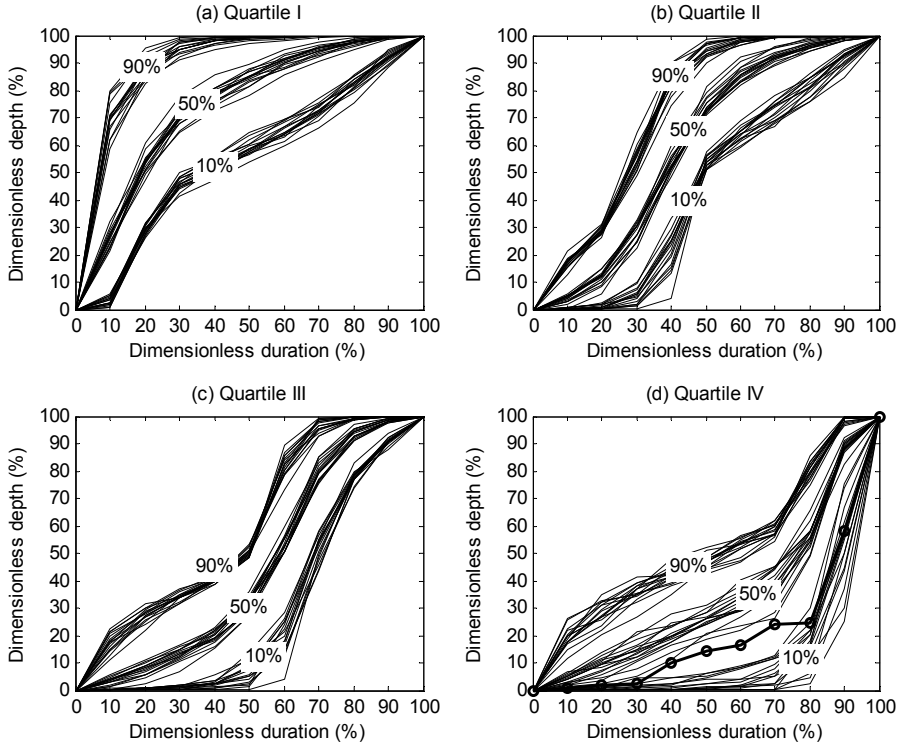

Figure 2. Huff curves for 10%, 50%, and 90% exceedance probabilities for the 18 stations for each storm type: (a) quartile I, (b) quartile II, (c) quartile III, and (d) quartile IV. Each solid line represents a station. The solid line with circles represents the 10% probability curve for Wuzhai station in Shanxi province.

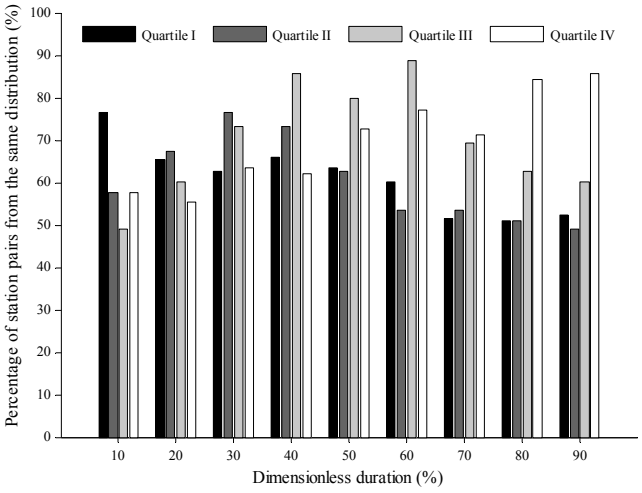

Figure 3. Station pairs from the same distribution based on two-sample Kolmogorov-Smirnov tests for nine representative dimensionless duration verticals.

that were statistically shown to be from the same distribution (*y*-axis, fig. 3) for a given peak quartile storm type (I to IV) tended to be greater for a dimensionless duration (*x*-axis) corresponding to or near when the peak occurred. For example, for quartile II storms (maximum rainfall in the 25% to 50% duration), the percentage of station pairs from the statistically similar distribution was greatest at 30% and 40% duration, which fell within the second quartile of the storm. For quartile III (maximum rainfall in the 50% to 75% duration), the greatest percentages of similar pairs appeared at 40%, 50%, and 60% durations.

The p-values of KS tests between station pairs were not significantly correlated with distances between stations (fig. 4), which suggested that station pairs close to each other did not demonstrate greater similarity of Huff curves compared to stations far from each other. The means ($\bar{p}_j$) and standard deviations (s'_j) of Huff curves across the 18 stations are shown in tables 3 and 4 to provide a reference for design storms and artificial storm experiments.

Quartile-Duration Relationship and Huff Curves for Different Durations

Of the storm events, 61.6% lasted for less than 24 h. The number of events shorter than 12 h was similar to the number between 12 and 24 h. Quartile I had the largest number and quartile IV had the least number of events for every storm duration category. However, the proportion of quartile I storms within each duration category decreased with increasing duration, whereas that for quartiles III and IV increased (fig. 5), showing that events of shorter duration were more strongly associated with peaks of rainfall in the front stages of the events.

Huff curves for different duration categories across four seasons for the four quartiles are shown in figure 6, taking 50% probability as an example. KS tests showed that the differences in the shapes of the curves were significant among duration categories, with quartiles I and IV being greater than those for quartiles II and III. KS tests showed that 85.2%, 74.1%, 54.8%, and 57.8% of duration group pairs were not from the same distribution for quartiles I, II, III, and IV, respectively. It is interesting to note that for quartile I, the curve for storms with shorter duration (e.g., ≤6 h) was shifted to the left of the other curves, indicating a more

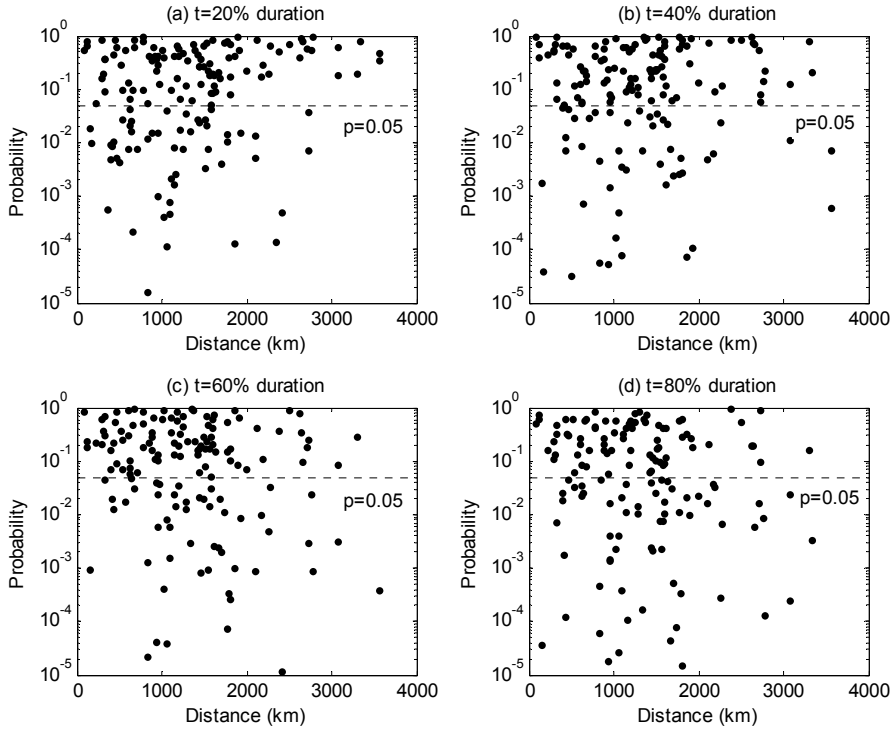

Figure 4. The p-values of two-sample Kolmogorov-Smirnov test related with distances between station pairs for quartile I storms for four representative dimensionless duration verticals: (a) t = 20% duration, (b) t = 40% duration, (c) t = 60% duration, and (d) t = 80% duration.

Table 3. Huff curve mean values for the four quartile classifications developed using all the storms from all 18 stations.

Duration	Quartile I			Quartile II		
(%)	10%	50%	90%	10%	50%	90%
0	0.0	0.0	0.0	0.0	0.0	0.0
10	3.5	26.6	71.4	0.3	3.9	17.6
20	29.5	54.5	88.9	1.0	11.3	28.9
30	46.1	70.9	95.8	4.6	28.3	55.6
40	52.7	79.3	98.2	21.0	53.8	83.7
50	59.1	85.3	99.0	54.1	75.3	94.9
60	65.8	90.7	99.4	64.5	86.4	98.4
70	72.9	94.7	99.7	72.7	92.6	99.4
80	82.0	97.5	99.8	81.7	96.6	99.7
90	91.7	99.2	99.9	91.8	99.0	99.9
100	100.0	100.0	100.0	100.0	100.0	100.0
	Quartile III			Quartile IV		
	10%	50%	90%	10%	50%	90%
0	0.0	0.0	0.0	0.0	0.0	0.0
10	0.2	3.1	17.6	0.3	3.8	18.9
20	0.5	7.3	27.0	0.6	8.3	27.3
30	1.0	12.5	33.7	1.1	13.4	35.1
40	2.1	19.1	39.9	2.0	18.6	40.6
50	5.8	30.7	49.7	3.1	24.3	46.3
60	19.1	53.5	82.4	4.5	29.4	52.3
70	50.9	79.8	96.4	7.0	36.8	57.7
80	77.8	93.4	99.3	17.0	55.0	79.4
90	90.9	98.5	99.8	49.3	88.3	98.7
100	100.0	100.0	100.0	100.0	100.0	100.0

Table 4. Huff curve standard deviations for the four quartile classifications developed using all the storms from all 18 stations.

Duration	Quartile I			Quartile II		
(%)	10%	50%	90%	10%	50%	90%
0	0.0	0.0	0.0	0.0	0.0	0.0
10	2.7	6.0	11.4	0.3	1.9	3.8
20	4.0	6.2	6.3	1.1	3.6	3.2
30	4.1	5.9	3.5	4.2	5.0	7.0
40	4.5	5.6	1.8	10.9	5.8	7.1
50	4.6	5.1	0.9	4.1	5.3	3.8
60	5.0	3.8	0.5	5.1	4.7	1.4
70	4.8	2.6	0.3	5.9	3.2	0.5
80	4.2	1.5	0.1	5.7	1.9	0.2
90	3.3	0.5	0.1	4.1	0.6	0.1
100	0.0	0.0	0.0	0.0	0.0	0.0
	Quartile III			Quartile IV		
	10%	50%	90%	10%	50%	90%
0	0.0	0.0	0.0	0.0	0.0	0.0
10	0.2	2.2	6.4	0.4	2.8	7.4
20	0.6	3.8	5.1	1.0	5.1	6.9
30	1.1	4.5	3.6	1.8	7.0	6.5
40	2.2	4.3	3.2	3.5	7.6	6.7
50	5.5	5.1	3.1	5.0	8.4	5.2
60	10.2	5.6	6.7	6.4	9.2	5.3
70	9.3	5.2	3.1	9.1	9.9	5.2
80	4.2	2.8	0.6	14.4	7.5	7.8
90	3.1	0.8	0.1	25.3	4.7	1.4
100	0.0	0.0	0.0	0.0	0.0	0.0

rapid normalized accumulation of dimensionless depth in the front stages of the events. Likewise, the curve for the longest storms (i.e., >48 h) was shifted to the right of the other storm durations. For quartile IV, the situation was exactly opposite, with dimensionless depth accumulating (normalized) more rapidly for the longer duration events in the front stages.

The percentage order for the four quartiles for summer is similar to that across all four seasons (i.e., for the entire year), which is quartile I, II, III, and IV in descending order. The percentages of shorter duration storms (≤6 h and 6 to 12 h) in quartiles I and II were greater for summer than for the four seasons combined. The effect of duration on the Huff curve shapes for summer is approximately the same as for the four seasons combined (not shown).

Quartile-Season Relationship and Huff Curves for Different Seasons

Figure 7 shows the percentage of storms in each quartile

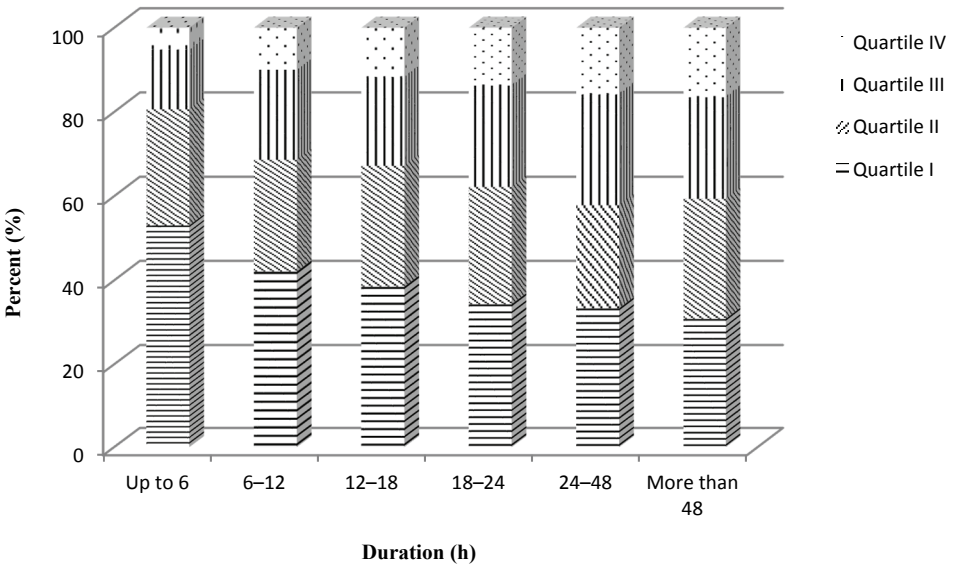

Figure 5. Percentage of storms in each quartile type as a function of duration category.

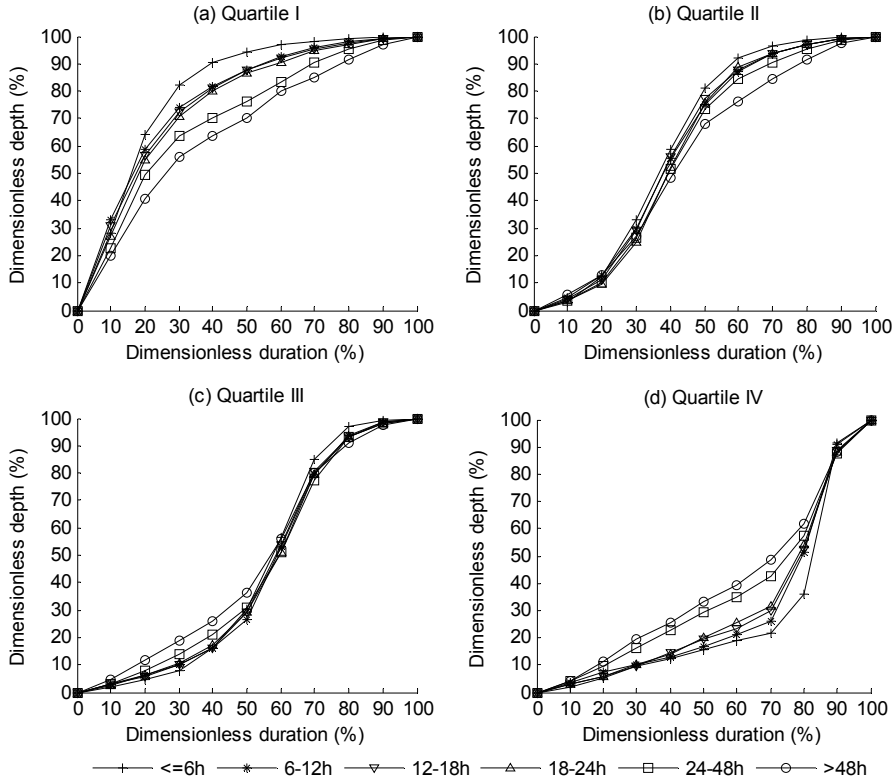

Figure 6. Huff curves (50% probability) for different duration categories across four seasons for (a) quartile I, (b) quartile II, (c) quartile III, and (d) quartile IV.

type as a function of season for all stations combined. The summer season (June through August) tended to have more quartile I and II storms, whereas the winter season (December through February) tended to have a more even distribution of storm quartile types, with approximately half of peaks occurring in the first half of the storm and half in the latter half.

Huff curves for the four seasons and the four quartiles are shown in figure 8, taking 50% probability as an example. As was the case for the differences in storm durations, the differences between the seasonal curves for quartiles I and IV were greater than those for quartiles II and III (fig. 8). For quartile I, the curve for summer storms was shifted to the left of the other curves, indicating a more rapid normalized accumulation of dimensionless depth in the front stages, and the curve for winter was shifted to the right of the other storm durations. For quartile IV, the summer events had dimensionless depth accumulating (normalized) more slowly than for the other seasons in the front stages.

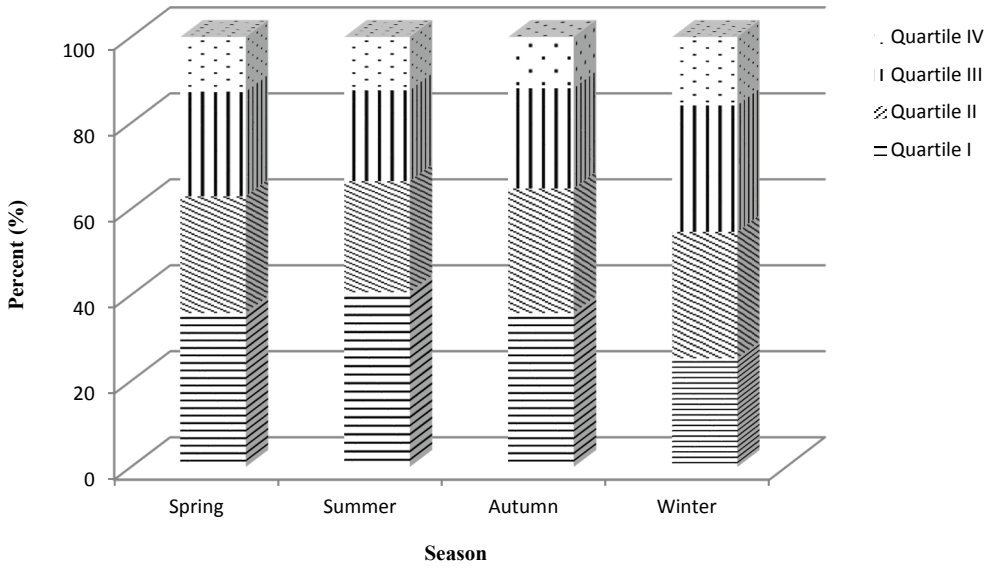

Figure 7. Percentage of storms in each quartile type for each season of the year.

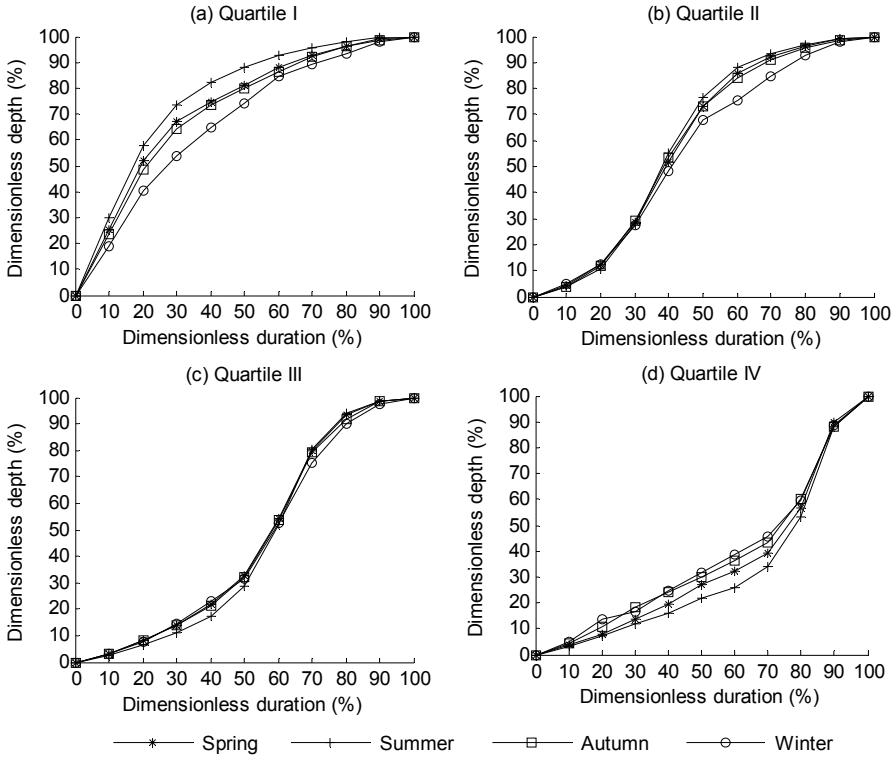

Figure 8. Huff curves (50% probability) for (a) spring, (b) summer, (c) autumn, and (d) winter.

CHARACTERISTICS OF STORMS FOR EACH QUARTILE TYPE

Storms that had the maximum rainfall occurring in the first and second quartiles tended to be of shorter duration and heavier intensity (table 5). The average rainfall amount for quartile I was 30.9 mm, and that for quartile IV was 31.8 mm. Two-sample t-tests showed that there were no statistically significant differences between these two means at a 5% significant level. However, differences in duration, I_{avg}, I_{30}, and EI_{30} between quartile I and IV storms were significant at the 5% level. Durations for quartile IV storms were 30% longer than the average for quartile I storms. The intensity and erosivity indices (I_{avg}, I_{30}, and EI_{30}) for quartile I storms were 1.71, 1.22, and 1.23 times greater

Table 5. Mean characteristics of storms for the four types of rain events averaged across all 18 stations.

Quartile	Amount (mm)	Duration (h)	I_{avg} (mm h^{-1})	I_{30} (mm h^{-1})	EI_{30} (MJ mm ha^{-1} h^{-1})
I	30.9	20.7	2.9	21.2	189.1
II	33.0	22.9	2.8	16.9	161.2
III	34.6	24.7	2.4	16.0	165.7
IV	31.8	27.0	1.7	17.3	153.6
Average	32.6	23.8	2.4	17.8	167.4

than those for quartile IV storms, respectively. Note that although the number of events and magnitude of event indices may change with the MDPD, the order of event statistics for different storm patterns was not expected to change as long as all storms were derived using the same MDPD criterion.

DISCUSSION

COMPARISONS BY STORM TYPE

A majority of past research has reported that the frequency of quartile I rainfall events is generally greater than that for other quartiles (Huff, 1990; Back, 2011; Bonnin et al., 2006, 2011; Perica et al., 2013a, 2013b). Our result also showed that the majority of storms overall were quartile I and that the fewest were quartile IV, which is consistent with Huff's research in Illinois and the Midwestern U.S. (Huff, 1990). For point rainfall, Huff found that quartile I rainfall events were the most frequent (37%), followed by rainfall events of quartile II (27%), quartile III (21%), and quartile IV (15%). In Urussange, Santa Catarina State, Brazil, it was found that the most frequent heavy rainfall events were of quartile I (42.4%), followed by quartile II (31.1%), quartile III (18.9%), and quartile IV (7.6%) (Back, 2011). For many parts of the U.S., research conducted by NOAA found that quartile I had the greatest number of events (Bonnin et al., 2006, 2011; Perica et al., 2013a, 2013b). For convective storms in the Midwestern states, 54% of storms belonged to quartile I (Bonnin et al., 2011). However, it was also pointed out that more front-loaded cases were due in part to the method for defining a precipitation event. In the NOAA studies, a precipitation case was defined as the total accumulation over a specific duration (6, 12, 24, or 96 h), in accordance with the methods used for NOAA's precipitation frequency analyses. As a result, the "event" always starts with precipitation but does not necessarily end with precipitation, so the percentage of quartile I would be expected to be larger compared to the single storm approach of Huff (1967).

Studies in other regions have reported quartile types other than quartile I as the predominant rainfall type. For peninsular Malaysia, the most frequent was quartile II (43%), followed by quartiles I (26%), III (22%), and IV (9%). The difference in that case may be partly due to the definition of events (Azli and Rao, 2010). In Huff (1967, 1990), Back (2011), and in this study, a minimum 6 h interval without precipitation was the criterion used for dividing two events, whereas Azli and Rao (2010) defined events as rainfall bursts with continuous rainfall and without necessarily any period of zero precipitation. Using that definition, 77.8% of events had a storm duration of less than 6 h. However, in this study, 12.3% of events had durations less than 6 h, and 31.2% had durations less than 12 h. For Santa Catarina in Brazil, 19.7% of events lasted less than 6 h, and 33.3% of events were less than 12 h (Back, 2011). For Illinois, Huff (1967) reported that 42% of events lasted less than 12 h.

For California (Perica et al., 2014), there was a tendency that the maximum frequency moved from the last quartile toward the earlier parts of the storm as duration increased from 6 to 96 h. When 14 regions in California were averaged, for up to 6 h rainfall, the most frequent type was quartile III (32.7%), followed by quartiles II (29.4%), IV (20.7%), and I (17.1%); for 6 to 12 h rainfall, quartiles II and III were the most prevalent; for 12 to 24 h, quartile II (30.4%) ranked first, and for 24 to 96 h, quartile I (33.4%) became the first.

COMPARISONS OF THE SHAPES OF THE PROBABILITY CURVES

Comparison of the 10%, 50%, and 90% probability curves from this study and with those reported for Illinois (Huff, 1990), peninsular Malaysia (Azli and Rao, 2010), and Santa Catarina in Brazil (Back, 2011) are shown in figures 9 and 10. The curves in this study were significantly different from those for the other areas. Statistical tests showed that 75.0%, 92.7%, and 63.9% of the representative duration verticals were significantly different when Huff curves in Illinois, peninsular Malaysia, and Santa Catarina were compared to those in this study, respectively (fig. 10). The differences were most apparent for the 90% and 50% probabilities for quartile I and the 50% and 10% probabilities for quartile IV, whereas curves for quartiles II and III demonstrated more similarities. Compared with those in the other regions, the curves in this study demonstrated the most variability in pattern, which means that the curves in this study were shifted to the left of the other curves for quartile I and they were shifted to the right for quartile IV.

The reason for the differences among Huff curves in this study and those from the other studies may be due to three aspects: (1) the definitions of individual storms and the criterion defining heavy storms for analysis, (2) the small number of storms sampled for curve development in some of the cases, and (3) differences in rainfall characteristics for different climatic areas. Each will be discussed here.

The first possible reason to explain the differences between our results and those of the other three studies is the definitions of individual storms and the criterion defining heavy storms for analysis. As mentioned in the previous section, the MDPD value delineating individual rain events was 6 h for Huff (1967, 1990), Back (2011), and this study, whereas no zero precipitation time in a storm was allowed by Azli and Rao (2010) when analyzing the data from peninsular Malaysia. Storms with mean amounts exceeding 12.7 mm and/or one or more stations over 25.4 mm were used by Huff (1967). Only storms with amounts for a station exceeding 25.4 mm were used by Azli and Rao (2010). An approach relating the amount with the duration was adopted by Back (2011), who used the criteria for defining heavy storms of 24.7, 32.4, and 38.4 mm for 1, 3, and 6 h duration storms, respectively.

In order to help understand these differences, a sensitivity analysis was done by comparing Huff curves developed from the storms delineated by five MDPD values (1, 3, 6, 9, and 12 h) using the data from this study. The result indicated (by visual inspection) that the curves based on an MDPD of 1 h were less like those based on the other MDPD values, especially for quartile IV storms (fig. 11). Huff curves developed based on storms with MDPD values of 3, 6, 9, and 12 h shared similar forms (fig. 11, visual inspection). Bonta and Rao (1987) indicated that Huff curves appear relatively insensitive to change in MDPD when curves were compared

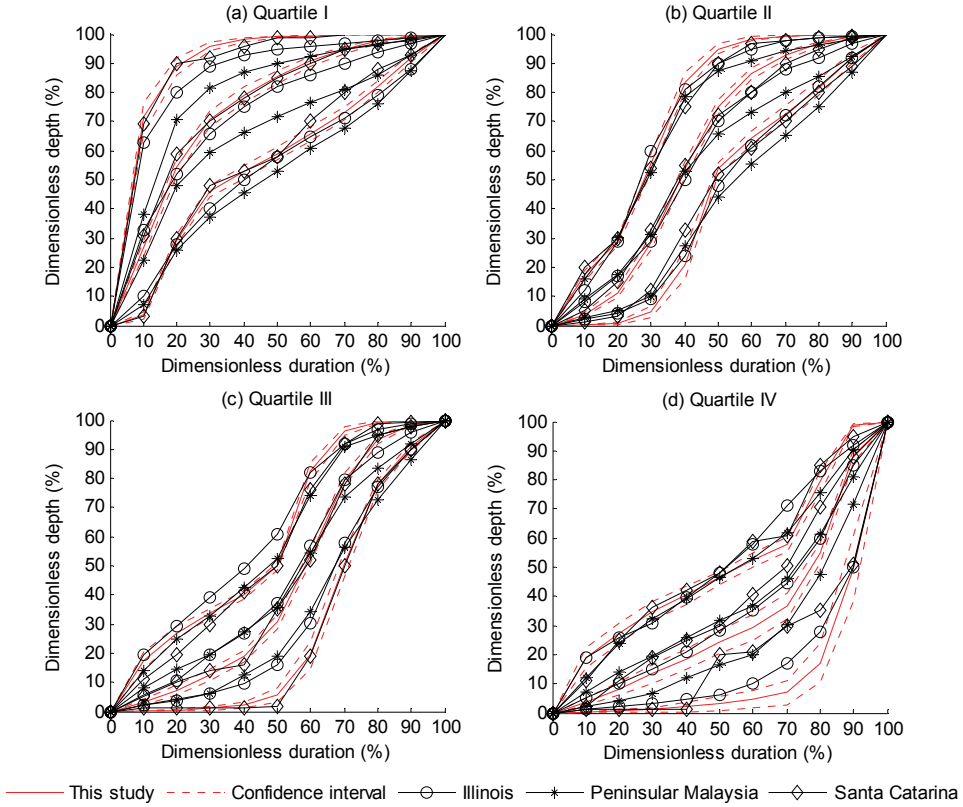

Figure 9. Comparison of curves for 10%, 50%, and 90% probabilities for Illinois (Huff, 1990), peninsular Malaysia (Azli and Rao, 2010), Santa Catarina in Brazil (Back, 2011), and the China data used in this study for each storm type: (a) quartile I, (b) quartile II, (c) quartile III, and (d) quartile IV.

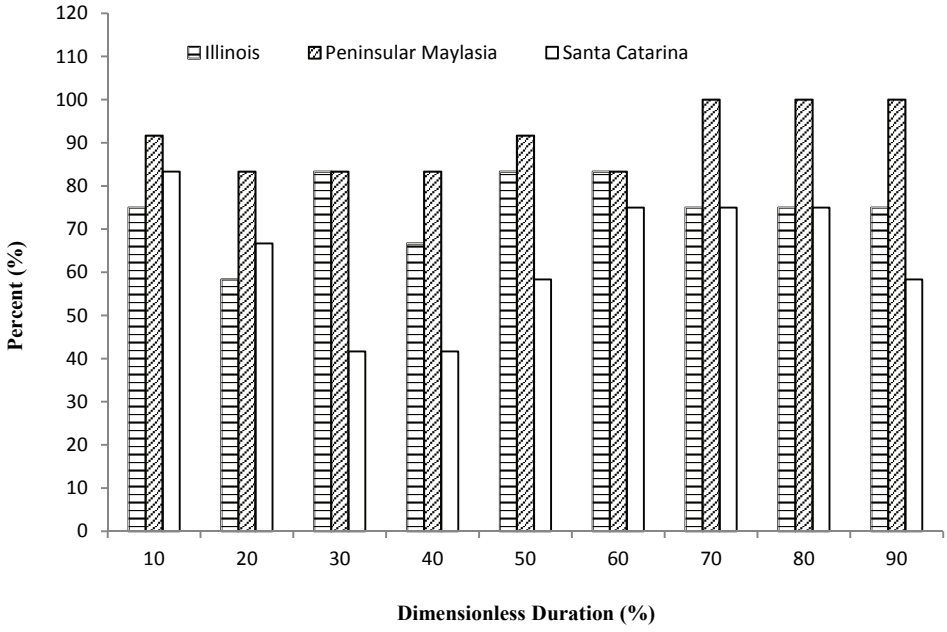

Figure 10. Percentage of tests with statistically different mean dimensionless depth of Huff curves for nine representative dimensionless duration verticals and three regions.

based on two MDPD values estimated by the rank correlation method (about 3 h) and the exponential method (about 9 h), respectively. Histograms of dry period durations between events were skewed right (Bonta and Rao, 1988b), which suggested that when the MDPD was larger (such as 3 h or more), the Huff curve patterns were less sensitive to the change in MDPD, which is similar to the result reported by Bonta and Rao (1987). Likewise, when the MDPD was smaller (such as 1 h or less), more difference in the storms was delineated, and the Huff curve patterns were more sen-

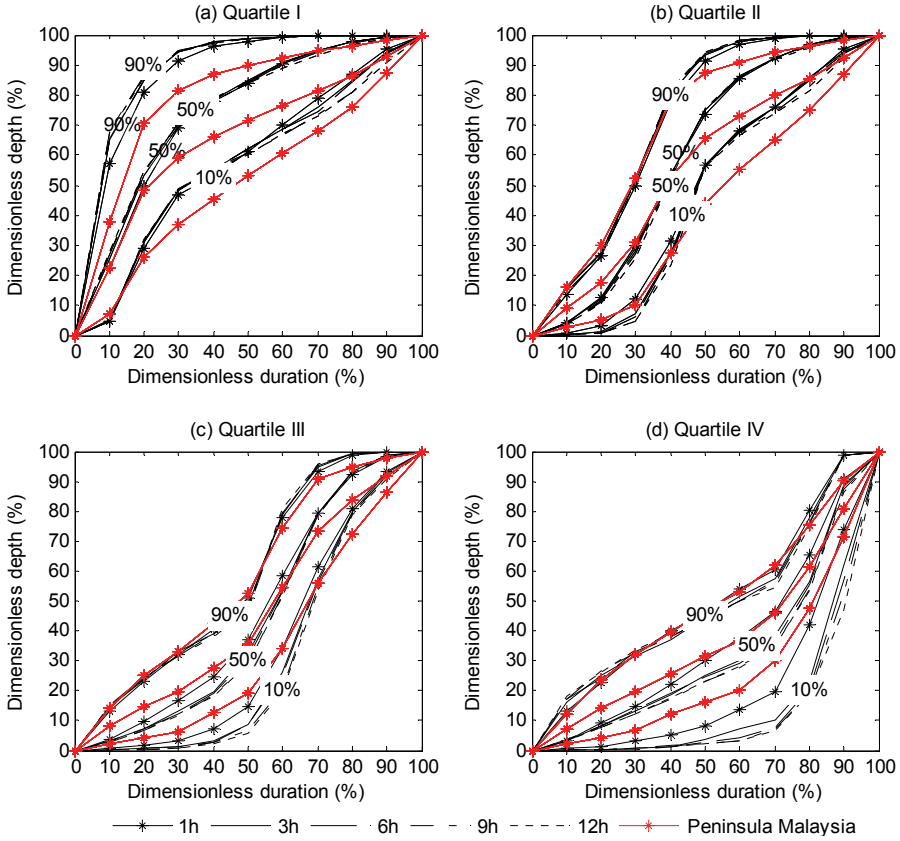

Figure 11. Comparison of averaged Huff curves for 18 stations developed based on the storms delineated by five minimum dry period duration (MDPD) values (1, 3, 6, 9, and 12 h) for (a) quartile I, (b) quartile II, (c) quartile III, and (d) quartile IV. Curves for peninsular Malaysia were from Azli and Rao (2010).

sitive to the change of MDPD. Differences between curves based on different storm amount criteria were negligible when 12.7 and 25.4 mm were compared (not shown). The differences between the curves developed in this study and those for peninsular Malaysia were the most apparent (fig. 9). Hourly rainfall data were used by Azli and Rao (2010) to develop the curves for peninsular Malaysia, so the MDPD can be assumed to be 1 h. The differences in Huff curves for MDPD of 1 h were less than those for MDPD of 6 h for this study when they were compared with the curves for peninsular Malaysia. However, the differences were still notable (fig. 11), which suggested that the definitions of individual storms explained part of the significant differences between the curves in this study and those of Azli and Rao (2010).

The second reason for the differences between the Huff curves in this study and those from the other locations may be the small number of storms sampled for curve development in some of the cases (Bonta and Rao, 1989). The 10% probability curve for quartile IV for Santa Catarina was not smooth (fig. 9), which may be due to the limited number of samples (ten for quartile IV). Recall that, in this study, the 10% exceedance curve for quartile IV for Wuzhai station was not smooth and fell relatively far from those for the other stations. The sample sizes for the other three quartiles for Santa Catarina were 56, 41, and 25, respectively. Bonta and Shahalam (2003) pointed out that a minimum sample size was needed when developing Huff curves. For example, they showed that more than 90 storms were needed using data from Coshocton, Ohio, and 120 storms were needed for an area in New Zealand, which suggested that the curves for Santa Catarina may be improved by using more storms.

The third important reason for the differences between the Huff curves in this study and those from the other locations may be the differences in rainfall characteristics for different climatic areas. The curves in this study shared more similar distributional characteristics with those of Santa Catarina in Brazil compared with those for Illinois and peninsular Malaysia. Both the southern region of Brazil, where Santa Catarina is located, and the central and eastern parts of China are greatly influenced by mid-latitude frontal systems, which may result in more similarities in the shape of Huff curves for these two regions. There is a tendency that quartile I rains are characteristically of shorter duration and higher intensity. This trend was evident in three ways in this study. First, the average duration for quartile I was about 3/4 of that for quartile IV, whereas the intensity indices for quartile I were 20% to 70% greater than those for quartile IV. Second, quartile-duration relationships showed that the proportion of quartile I decreased with longer durations, whereas the proportions of quartiles III and IV increased. Third, quartile I occurred more frequently in summer, whereas the percentage of quartile I was lower than that of quartiles II and III in winter. Comparison of Huff curves for different durations and different seasons also suggested that storms with shorter duration tended to show more variability

in pattern compared to storms with longer durations. Rainstorms in summer in China mainly arise from convective processes and cold fronts (Wang and Li, 2007). Convective rains characterized by shorter duration and heavier intensity tend to start suddenly and generate maximum rain in the first half of the storm, which may partly explain the variability in pattern of the Huff curves for China.

Comparisons on the Quartile-Duration and Quartile-Season Relationships

The quartile-duration relationships in this study were consistent with Huff (1967), which showed that first and second quartile storms most often had durations of less than 12 h, and third and fourth quartile storms occurred most frequently in the 12 to 24 h and greater than 24 h duration groups, respectively. Bonta (2004a) suggested that storms need to be categorized by month when quartile-duration relationships are analyzed due to different storm-duration characteristics in different seasons. In this study, the difference in quartile-duration relationships was that shorter-duration storms were more concentrated in quartiles I and II, and the difference in the effect of duration on the shapes of Huff curves between the summer season and the entire year combined was negligible. The main reason for this may be due to the fact that most erosive storms (56.4%) occurred in summer in the monsoon climate in the central and eastern parts of China, which resulted in the effect of duration on curves being dominated by summer storms. A significant effect of season on Huff curves was also shown by Bonta (2004a), which supported the idea that Huff curves should be developed for different seasons of the year.

Climate Change Considerations

The global hydrologic cycle has tended to be more active due to the increasing global surface temperatures over the 20th century (Dore, 2005; Groisman et al., 2005). Heavy precipitation has shown an increasing trend for many mid-latitude regions (IPCC, 2007). Some research has focused on the trends of intra-storm characteristics. For example, research conducted by Yin et al. (2011) demonstrated that the mean intensities and peak intensities have increased and the time to peak intensity has become earlier for short-duration events in the Haihe River basin in China during the last several decades. An increasing risk of urban waterlogging, local flooding, and soil erosion has emerged. The changing trends in intra-storm characteristics reflected by Huff curves in the context of climate change and their impacts on drainage design and soil erosion risk assessment are worth investigating. Calibrated hydrologic and erosion models could be used to determine how runoff and erosion amounts are affected by using different Huff curves as inputs to the models.

Conclusions

A total of 11,801 erosive events from 18 weather stations with 1 min resolution data were analyzed to generate Huff curves for the eastern and central parts of China. The following conclusions can be presented:

- On average, 38.3% of the storms were quartile I, followed by quartiles II (26.8%), III (22.4%), and IV (12.5%). More than half of the erosive events occurred in summer (June through August), with 40.8% of them being quartile I and 25.9% being quartile II.
- The curves for different stations shared similarities, and the station pairs near to each other did not show greater similarity of Huff curves compared to those far from each other. Regional Huff curves, including means and standard deviations based on a bootstrap scheme, were presented.
- Storms that had the maximum rainfall occurring in the first and second quartiles tended to be characterized by shorter duration and heavier intensity. The average duration for quartile I was about 3/4 of that for quartile IV, whereas the intensity indices for quartile I were 20% to 70% more than those of quartile IV. Huff curves derived from storms with shorter durations demonstrated more variability in pattern.
- Huff curves for Illinois, peninsular Malaysia, and Santa Catarina in Brazil reported in previous studies exhibited dissimilarities both in terms of the percentages of storms of various quartile classifications and the curve shapes compared with the Huff curves developed for China in this study. The reasons for this are due to both differences in data analysis methods and climate between locations.

The significant differences in rainfall characteristics among different types of rainfall suggest that more attention should be paid to rainstorm type and intra-storm characteristics when infiltration processes are considered and modeled. Huff curves reflect intra-storm temporal rainfall characteristics, and they can be useful for drainage design in urban areas as well as runoff and erosion simulations in rural areas.

Acknowledgements

The authors would like to thank the Heilongjiang, Shanxi, Shaanxi, Beijing, Sichuan, Hubei, Fujian, and Yunnan Meteorological Bureaus for supplying rainfall data. This work was supported by National Natural Science Foundation of China (No. 41301281) and China Special Fund for Meteorological Research in the Public Interest (GYHY201506014). Thanks to James V. Bonta for his advice.

References

Al-Rawas, G. A., & Valeo, C. (2009). Characteristics of rainstorm temporal distributions in arid mountainous and coastal regions. *J. Hydrol., 376*(1-2), 318-326. http://dx.doi.org/10.1016/j.jhydrol.2009.07.044

Azli, M., & Rao, A. R. (2010). Development of Huff curves for peninsular Malaysia. *J. Hydrol., 388*(1-2), 77-84. http://dx.doi.org/10.1016/j.jhydrol.2010.04.030

Back, A. J. (2011). Time distribution of heavy rainfall events in Urussanga, Santa Catarina State, Brazil. *Acta Sci. Agron., 33*(4), 583-588. https://doi.org/10.4025/actasciagron.v33i4.6664

Bonnin, G. M., Martin, D., Lin, B., Parzybok, T., Yekta, M., & Riley, D. (2006). *NOAA atlas 14: Precipitation frequency atlas of the United States* (Vol. 2). Silver Spring, MD: NOAA.

Bonnin, G. M., Martin, D., Lin, B., Parzybok, T., Yekta, M., & Riley, D. (2011). *NOAA atlas 14: Precipitation frequency atlas*

of the United States (Vol. 1). Silver Spring, MD: NOAA.
Bonta, J. V. (2004a). Development and utility of Huff curves for disaggregating precipitation amounts. *Appl. Eng. Agric., 20*(5), 641-653. http://dx.doi.org/10.13031/2013.17467
Bonta, J. V. (2004b). Stochastic simulation of storm occurrence, depth, duration, and within-storm intensities. *Trans. ASAE, 47*(5), 1573-1584. http://dx.doi.org/10.13031/2013.17635
Bonta, J. V., & Rao, A. R. (1987). Factors affecting development of Huff curves. *Trans. ASAE, 30*(6), 1689-1693. http://dx.doi.org/10.13031/2013.30623
Bonta, J. V., & Rao, A. R. (1988a). Comparison of four design-storm hyetographs. *Trans. ASAE, 31*(1), 102-106. http://dx.doi.org/10.13031/2013.30673
Bonta, J. V., & Rao, A. R. (1988b). Factors affecting the identification of independent storm events. *J. Hydrol., 98*(3), 275-293. http://dx.doi.org/10.1016/0022-1694(88)90018-2
Bonta, J. V., & Rao, A. R. (1989). Regionalization of storm hyetographs. *Water Resour. Bull., 25*(1), 211-217. http://dx.doi.org/10.1111/j.1752-1688.1989.tb05683.x
Bonta, J. V., & Shahalam, A. (2003). Cumulative storm rainfall distributions: Comparison of Huff curves. *J. Hydrol. New Zealand, 42*(1), 65-74.
Dore, M. H. I. (2005). Climate change and changes in global precipitation patterns: What do we know? *Environ. Intl., 31*(8), 1167-1181. http://dx.doi.org/10.1016/j.envint.2005.03.004
Dunkerley, D. (2012). Effects of rainfall intensity fluctuations on infiltration and runoff: Rainfall simulation on dryland soils, Fowlers Gap, Australia. *Hydrol. Proc., 26*(15), 2211-2224. http://dx.doi.org/10.1002/hyp.8317
Fan, Z. H. (2011). Research on precipitation trend analysis and design storm of Tianjin city [in Chinese]. MS thesis. Tianjin, China: Tianjin University.
Flanagan, D. C., Foster, G. R., & Moldenhauer, W. C. (1988). Storm pattern effect on infiltration, runoff, and erosion. *Trans. ASAE, 31*(2), 414-420. http://dx.doi.org/10.13031/2013.30724
Foster, G. R. (2004). User's reference guide: Revised Universal Soil Loss Equation (RUSLE2). Washington, DC: USDA-ARS.
Groisman, P. Y., Knight, R. W., Easterling, D. R., Karl, T. R., Hegerl, G. C., & Razuvaev, V. A. N. (2005). Trends in intense precipitation in the climate record. *J. Climate, 18*(9), 1326-1350. http://dx.doi.org/10.1175/jcli3339.1
Hershfield, D. M. (1962). Extreme rainfall relationships. *J. Hydraul. Div., 88*(6), 73-92.
Hjelmfelt, A. T. (1980). Time distribution of clock hour rainfall. In W. D. Knisel (Ed.), *CREAMS: A field-scale model for chemicals, runoff, and erosion from agriculture management systems*. Conservation Research Report No. 26. Washington, DC: USDA.
Huff, F. A. (1967). Time distribution of rainfall in heavy storms. *Water Resour. Res., 3*(4), 1007-1019. http://dx.doi.org/10.1029/WR003i004p01007
Huff, F. A. (1990). Time distributions of heavy rainstorms in Illinois. Circular 173. Champaign, IL: Illinois State Water Survey.
IPCC. (2007). Summary for policymakers. In S. Solomon, D. Qin, M. Manning, Z. Chen, M. Marquis, K. B. Averyt, ... H. L. Miller (Eds.), *Climate Change 2007: The Physical Science Basis, Contribution of Working Group I to the Fourth Assessment Report of the Intergovernmental Panel on Climate Change*. Cambridge, UK: Cambridge University Press.
Kandel, D. D., Western, A. W., Grayson, R. B., & Turral, H. N. (2004). Process parameterization and temporal scaling in surface runoff and erosion modelling. *Hydrol. Proc., 18*(8), 1423-1446. http://dx.doi.org/10.1002/hyp.1421
Keifer, C. J., & Chu, H. H. (1957). Synthetic storm pattern for drainage design. *J. Hydraul. Div., 83*(4), 1-25.
Lane, L. J., & Nearing, M. A. (1989). USDA Water Erosion Prediction Project: Hillslope profile and watershed model documentation. West Lafayette, IN: USDA-ARS National Soil Erosion Research Laboratory.
Loukas, A., & Quick, M. C. (1996). Spatial and temporal distribution of storm precipitation in southwestern British Columbia. *J. Hydrol., 174*(1), 37-56. http://dx.doi.org/10.1016/0022-1694(95)02754-8
NERC. (1975). *Flood studies report, Vol. II: Meteorological studies*. London, UK: Natural Environment Research Council.
Perica, S., Dietz, S., Heim, S., Hiner, L., Maitaria, K., Martin, D., ... Yarchoan, J. (2014). *NOAA atlas 14: Precipitation frequency atlas of the United States* (Vol. 6). Silver Spring, MD: NOAA.
Perica, S., Martin, D., Pavlovic, S., Roy, I., St. Laurent, M., Trypaluk, C., ... Bonnin, G. (2013a). *NOAA atlas 14: Precipitation frequency atlas of the United States* (Vol. 8). Silver Spring, MD: NOAA.
Perica, S., Martin, D., Pavlovic, S., Roy, I., St. Laurent, M., Trypaluk, C., ... Bonnin, G. (2013b). *NOAA atlas 14: Precipitation frequency atlas of the United States* (Vol. 9). Silver Spring, MD: NOAA.
Pilgrim, D. H., & Cordery, I. (1975). Rainfall temporal patterns for design floods. *J Hydraul. Div., 101*(1), 81-95.
Renard, K. G., Foster, G. R., Weesies, G., ... McCool, D. K., & Yoder, D. C. (1997). Predicting soil erosion by water. Agriculture Handbook 703. Washington, DC: USDA-ARS.
Ross, P. J. (1990). SWIM: A simulation model for soil water infiltration and movement. Townsville, Queensland, Australia: CSIRO Division of Soils.
Snedecor, G. W., & Cochran, W. G. (1989). *Statistical methods* (8th ed.). Ames, IA: Iowa State Univeristy Press.
Terranova, O. G., & Iaquinta, P. (2011). Temporal properties of rainfall events in Calabria (southern Italy). *Nat. Hazards Earth Syst. Sci., 11*(3), 751-757. http://dx.doi.org/10.5194/nhess-11-751-2011
USDA. (1986). Urban hydrology for small watersheds. Technical Release 55. Washington, DC: USDA Soil Conservation Service.
Wang, B. M., Lu, Y., & Zhang, Q. (2004). The color scanning digitizing processing system of precipitation autographic record paper [in Chinese]. *J Appl. Meteorol. Sci., 15*(6), 737-744.
Wang, J. Q. (2002). *Rainstorms in China* [in Chinese]. Beijing, China: China Water Power.
Wang, M., & Tan, X. (1994). A study on storm and rainfall pattern in Beijing city [in Chinese]. *J. China Hydrol.*(3), 1-6.
Wang, S. W., & Li, W. J. (2007). *Climate of China*. Beijing, China: China Meteorological Press.
Wischmeier, W. H., & Smith, D. D. (1978). Predicting rainfall erosion losses: A guide to conservation planning. Agriculture Handbook 537. Washington, DC: USDA-ARS.
Wu, S. (2002). Analysis of rainfall characteristics and experimental study of runoff-producing and flow concentration characteristics of city's underlying surface in Xi'an [in Chinese]. MS thesis. Xi'an, China: Xi'an University of Technology.
Xie, Y., Liu, B., & Nearing, M. A. (2002). Practical thresholds for separating erosive and non-erosive storms. *Trans. ASAE, 45*(6), 1843-1847. http://dx.doi.org/10.13031/2013.11435
Yen, B. C., & Chow, V. T. (1980). Design hyetographs for small drainage structures. *J. Hydraul. Div., 106*(6), 1055-1076.
Yin, S. Q., Gao, G., Li, W. J., Chen, D., & Hao, L. S. (2011). Long-term precipitation change by hourly data in Haihe River basin during 1961-2004. *Sci. China Earth Sci., 54*(10), 1576. http://dx.doi.org/10.1007/s11430-011-4232-z
Yu, B., Rose, C., Coughlan, K., & Fentie, B. (1997). Plot-scale rainfall-runoff characteristics and modeling at six sites in Australia and Southeast Asia. *Trans. ASAE, 40*(5). http://dx.doi.org/10.13031/2013.21387